Interaction of ^{11}C-Tariquidar and ^{11}C-Elacridar with P-Glycoprotein and Breast Cancer Resistance Protein at the Human Blood–Brain Barrier

Martin Bauer[1], Rudolf Karch[2], Markus Zeitlinger[1], Johann Stanek[1,3], Cécile Philippe[1,4], Wolfgang Wadsak[4], Markus Mitterhauser[4], Walter Jäger[5], Helmuth Haslacher[6], Markus Müller[1], and Oliver Langer[1,3]

[1]Department of Clinical Pharmacology, Medical University of Vienna, Vienna, Austria; [2]Center for Medical Statistics, Informatics, and Intelligent Systems, Medical University of Vienna, Vienna, Austria; [3]Health and Environment Department, AIT Austrian Institute of Technology GmbH, Seibersdorf, Austria; [4]Department of Nuclear Medicine, Medical University of Vienna, Vienna, Austria; [5]Department of Clinical Pharmacy and Diagnostics, University of Vienna, Vienna, Austria; and [6]Department of Laboratory Medicine, Medical University of Vienna, Vienna, Austria

The adenosine triphosphate-binding cassette transporters P-glycoprotein (Pgp) and breast cancer resistance protein (BCRP) are 2 major gatekeepers at the blood–brain barrier (BBB) that restrict brain distribution of several clinically used drugs. In this study, we investigated the suitability of the radiolabeled Pgp/BCRP inhibitors ^{11}C-tariquidar and ^{11}C-elacridar to assess Pgp density in the human brain with PET. **Methods:** Healthy subjects underwent a first PET scan of 120-min duration with either ^{11}C-tariquidar ($n = 6$) or ^{11}C-elacridar ($n = 5$) followed by a second PET scan of 60-min duration with (*R*)-^{11}C-verapamil. During scan 1 (at 60 min after radiotracer injection), unlabeled tariquidar (3 mg/kg) was intravenously administered. Data were analyzed using 1-tissue 2-rate-constant (1T2K) and 2-tissue 4-rate-constant (2T4K) compartment models and either metabolite-corrected or uncorrected arterial input functions. **Results:** After injection of ^{11}C-tariquidar or ^{11}C-elacridar, the brain PET signal corrected for radioactivity in the vasculature was low (~0.1 standardized uptake value), with slow washout. In response to tariquidar injection, a moderate but statistically significant rise in brain PET signal was observed for ^{11}C-tariquidar (+27% ± 15%, $P = 0.014$, paired *t* test) and ^{11}C-elacridar (+21% ± 15%, $P = 0.014$) without changes in plasma activity concentrations. Low levels of radiolabeled metabolites (<25%) were detected in plasma up to 60 min after injection of ^{11}C-tariquidar or ^{11}C-elacridar. The 2T4K model provided better data fits than the 1T2K model. Model outcome parameters were similar when metabolite-corrected or uncorrected input functions were used. There was no significant correlation between distribution volumes of ^{11}C-tariquidar or ^{11}C-elacridar and distribution volumes of (*R*)-^{11}C-verapamil in different brain regions. **Conclusion:** The in vivo behavior of ^{11}C-tariquidar and ^{11}C-elacridar was consistent with that of dual Pgp/BCRP substrates. Both tracers were unable to visualize cerebral Pgp density, most likely because of insufficiently high binding affinities in relation to the low density of Pgp in human brain (~1.3 nM). Despite their inability to visualize Pgp density, ^{11}C-tariquidar and ^{11}C-elacridar may find use as a new class of radiotracers to study the interplay of Pgp and BCRP at the human BBB in limiting brain uptake of dual substrates.

Received Dec. 7, 2012; revision accepted Apr. 19, 2013.

For correspondence or reprints contact: Oliver Langer, Department of Clinical Pharmacology, Medical University of Vienna, Währinger-Gürtel 18-20, 1090 Vienna, Austria.

E-mail: oliver.langer@meduniwien.ac.at

Published online Jul. 5, 2013

Key Words: P-glycoprotein; breast cancer resistance protein; blood-brain barrier; ^{11}C-tariquidar; ^{11}C-elacridar

J Nucl Med 2013; 54:1181–1187
DOI: 10.2967/jnumed.112.118232

The adenosine triphosphate–binding cassette (ABC) transporters P-glycoprotein (Pgp) and breast cancer resistance protein (humans: BCRP; rodents: Bcrp) act together as a team of gatekeepers at the blood–brain barrier (BBB) at the level of the luminal (blood-facing) membrane of vascular endothelial cells to protect the brain from the accumulation of mostly lipophilic xeno- and endobiotics (*1*). Various clinically used drugs, most notably several members of the family of tyrosine kinase inhibitors for cancer treatment (e.g., gefitinib, imatinib, and sorafenib), were shown to be dual substrates of Pgp and BCRP (*1*). It has been demonstrated that Pgp and BCRP form a cooperative drug efflux system at the BBB and that dual substrates gain brain access only when both transporters are genetically or chemically disrupted (*2*). Tariquidar and elacridar are potent third-generation inhibitors of Pgp that were later discovered to also inhibit BCRP, albeit at higher concentrations than Pgp (*3*). Based on the assumption that tariquidar and elacridar would bind to Pgp without being transported (*4*), ^{11}C-tariquidar and ^{11}C-elacridar were developed as PET tracers to visualize Pgp expression levels at the BBB as opposed to substrates, such as ^{11}C-verapamil or ^{11}C-*N*-desmethyl-loperamide, which visualize Pgp function (*5*). However, initial preclinical evaluation revealed that baseline brain uptake of ^{11}C-tariquidar and ^{11}C-elacridar was low in rats or mice and significantly increased in Pgp/Bcrp combination knockout mice or after pretreatment of animals with unlabeled tariquidar or elacridar (*6–9*). This "substratelike" in vivo behavior was subsequently confirmed in vitro by showing that both tariquidar and elacridar are avidly transported by Pgp and BCRP in nanomolar concentrations as used for PET (*10,11*). On the other hand, PET experiments in a low- and high-Pgp-expressing murine breast tumor graft model showed higher uptake of ^{11}C-tariquidar in Pgp-overexpressing tumors, consistent with Pgp binding (*12*). Similarly, paired PET scans with ^{11}C-tariquidar or ^{11}C-elacridar and (*R*)-^{11}C-verapamil in naïve rats, with an intravenous administration of tariquidar (3 mg/kg)

before the (*R*)-^{11}C-verapamil scan, revealed a significant negative correlation between regional brain distribution volumes (V_Ts) of ^{11}C-tariquidar or ^{11}C-elacridar and (*R*)-^{11}C-verapamil, which also pointed to Pgp-specific binding of ^{11}C-tariquidar and ^{11}C-elacridar (*13*). Such a paired-scan protocol could in theory be used to independently assess Pgp expression and Pgp function in a single scan session.

The aim of this study was to investigate the suitability of ^{11}C-tariquidar and ^{11}C-elacridar for visualizing cerebral Pgp density in healthy human subjects. In analogy to a previous preclinical study (*13*) we performed paired PET scans with ^{11}C-tariquidar or ^{11}C-elacridar and (*R*)-^{11}C-verapamil including a pharmacologic challenge with tariquidar (3 mg/kg).

MATERIALS AND METHODS

Subjects

The study was conducted in accordance with the Declaration of Helsinki and its amendments, registered with European Union Drug Regulating Authorities Clinical Trials (number 2010-020759-30), and approved by the Ethics Committee of the Medical University of Vienna. The study was conducted as a prospective single-center, randomized phase I study. All subjects provided written informed consent and were confirmed to be healthy on the basis of medical history, physical examination, routine laboratory tests, urine drug screening, electrocardiography, and vital signs. Eleven healthy men (mean age, 34 ± 8 y; mean weight, 76 ± 10 kg) were randomly assigned to receive either an ^{11}C-tariquidar ($n = 6$) or an ^{11}C-elacridar ($n = 5$) PET scan followed by an (*R*)-^{11}C-verapamil PET scan (Fig. 1).

Radiotracer Synthesis

^{11}C-tariquidar, ^{11}C-elacridar, and (*R*)-^{11}C-verapamil were synthesized following previously published procedures (*8,9,14*) and formulated in 20-mL sterile 0.9% (w/v) aqueous saline solution/ethanol (9/1, v/v) (containing 1.4% [v/v] polysorbate-80 in the case of ^{11}C-tariquidar and ^{11}C-elacridar). Radiotracer solutions were sterilized by passage through sterile Millex-GV filters (0.22 μm) (Millipore). Polysorbate-80 was used as an excipient to prevent nonspecific binding of radiotracers to filter membranes. Polysorbate-80 has been reported to inhibit Pgp with a half-maximum inhibitory concentration of 24 μM (*15*). In a previous preclinical study, we administered polysorbate-80 at doses of up to 0.3 mmol/kg and failed to observe a Pgp inhibitory effect at the BBB (*16*). Specific activities at the time of injection were 19 ± 7, 42 ± 20, and 38 ± 18 GBq/μmol for ^{11}C-tariquidar (6 batches), ^{11}C-elacridar (5 batches), and (*R*)-^{11}C-verapamil (10 batches), respectively. The radiochemical purity of all radiotracers was greater than 98%.

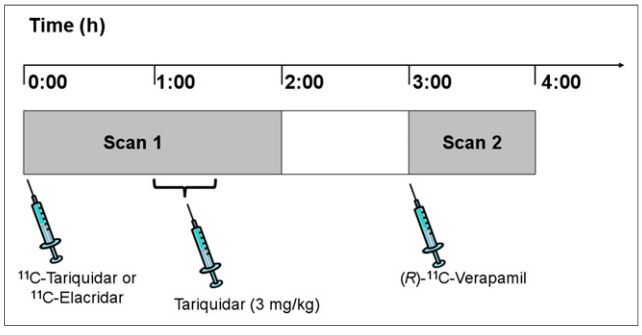

FIGURE 1. Diagram of study set-up. PET scan 1 with either ^{11}C-tariquidar or ^{11}C-elacridar over 120 min was followed by PET scan 2 with (*R*)-^{11}C-verapamil over 60 min with interval of 60 min between the 2 scans. At 60 min after start of scan 1, unlabeled tariquidar was infused intravenously at dose of 3 mg/kg over 30 min.

PET Study Protocol

The subjects underwent a first PET scan of 120-min duration with either ^{11}C-tariquidar or ^{11}C-elacridar followed by a second PET scan of 60-min duration with (*R*)-^{11}C-verapamil, with 1 h between the 2 scans (Fig. 1). During scan 1 (at 60 min after tracer injection), tariquidar (AzaTrius Pharmaceuticals Pvt Ltd.) was administered at a dose of 3 mg/kg of body weight (3.6 μmol/kg) as an intravenous infusion over 30 min. For formulation of the infusion solution, a 7.5 mg/mL stock solution of tariquidar (free base) in 20% ethanol/80% propylene glycol was diluted in aqueous dextrose solution (5%, w/v) to a final volume of 250 mL.

PET Scans

All PET scans were obtained on an Advance scanner run in 3-dimensional mode (GE Healthcare). For scan 1, either ^{11}C-tariquidar (5.0 ± 0.8 MBq/kg, corresponding to 0.3 ± 0.1 nmol of unlabeled tariquidar and 1.2 ± 0.8 μmol of polysorbate-80 per kilogram) or ^{11}C-elacridar (5.0 ± 0.5 MBq/kg, corresponding to 0.2 ± 0.1 nmol of unlabeled elacridar and 0.5 ± 0.2 μmol of polysorbate-80 per kilogram) was intravenously injected over 30 s, and dynamic emission scans were acquired for 120 min in 26 frames of increasing duration from 15 s to 10 min. For scan 2, (*R*)-^{11}C-verapamil (5.1 ± 0.7 MBq/kg, corresponding to 0.2 ± 0.1 nmol of unlabeled (*R*)-verapamil per kilogram) was injected over 30 s, and dynamic emission scans were acquired for 60 min in 20 frames of increasing duration from 15 s to 10 min. Before each radiotracer injection, a 5-min transmission scan using two ^{68}Ge pin sources was recorded.

Safety Monitoring

All subjects were monitored for the safety parameters heart rate and blood pressure until they were discharged from the study ward the morning after the PET scan. In addition, clinical laboratory blood and urine tests were performed. Adverse events were recorded continuously, and the relationship to the study drugs was assessed.

Blood Analysis

To determine the arterial input function of ^{11}C-tariquidar and ^{11}C-elacridar, blood samples (2 mL each) were manually drawn from the radial artery at 7-s intervals for the first 2 min, followed by samples at 3.5, 5, and 10 min (9 mL each); at 20, 30, 40, and 60 min (18 mL each); and at 75, 90, 105, and 120 min (9 mL each) after radiotracer injection. Aliquots of blood and plasma were measured for radioactivity in a γ-counter, which was cross-calibrated with the PET camera. Plasma samples collected at 3.5, 5, 10, 20, 30, 40, and 60 min were analyzed for radiolabeled metabolites of ^{11}C-tariquidar and ^{11}C-elacridar using a previously developed solid-phase extraction (SPE) assay (*8*). In brief, plasma (2–4 mL) was diluted with water (2 mL), spiked with unlabeled elacridar or tariquidar (10 μL, 20 mg/mL in dimethylsulfoxide), acidified with 5 M aqueous hydrochloric acid (40 μL), and loaded on a Sep-Pak vac tC18 cartridge (Waters Corp.), which had been preactivated with methanol (3 mL) and water (5 mL). The cartridge was first washed with water (5 mL) and then eluted with methanol (2 mL) followed by aqueous ammonium acetate buffer (0.2 M, pH 5.0, 1.5 mL). Radioactivity in all 3 fractions (plasma, water, and methanol/buffer) was quantified in a γ-counter. Radioactivity in the plasma and water fractions contained polar radiolabeled metabolites, whereas unchanged ^{11}C-tariquidar and ^{11}C-elacridar were recovered in the methanol/buffer fraction. Recoveries of ^{11}C-tariquidar and ^{11}C-elacridar from the methanol/buffer fraction of the SPE assay ranged from 91% to 94%. The methanol/buffer fractions from 10-, 20-, 30-, 40-, and 60-min samples were further analyzed for radiolabeled metabolites of ^{11}C-tariquidar and ^{11}C-elacridar by reversed-phase

high-performance liquid chromatography (HPLC) using a binary gradient system (Supplemental Fig. 2 shows HPLC conditions; supplemental materials are available at http://jnm.snmjournals.org). Plasma input functions of ^{11}C-tariquidar and ^{11}C-elacridar were constructed by multiplying total activity concentrations in whole blood (from 0 to 60 min) with the mean ratios of plasma to whole-blood activity (determined from 3.5-, 5-, 10-, 20-, 30-, 40-, and 60-min blood samples) with or without correcting for the fraction of polar radiolabeled metabolites, as determined by SPE, and by subsequent linear interpolation of the activity data. Blood sampling, metabolite analysis, and input function generation for the (*R*)-^{11}C-verapamil scan were performed as described previously (*14,17*). In addition, 4 venous 4-mL blood samples were collected from each subject at the end of the tariquidar infusion, at the end of the first PET scan, and at the beginning and end of the second PET scan to measure tariquidar plasma concentration levels using a previously described liquid chromatography–tandem mass spectrometry assay (*18*).

Image Analysis

T1-weighted MR images, acquired with an Achieva 3.0-T scanner (Philips), and the corresponding PET data were processed with Analyze 8.0 (Biomedical Imaging Resource; Mayo Foundation) and SPM5 (Wellcome Department of Imaging Neuroscience; University College London) software as described previously (*14*). By using the Hammersmith n30r83 3-dimensional maximum probability atlas of the human brain (*19*), we were able to apply a template of preset volumes of interest to the PET images to extract time–activity curves for the following 7 gray matter regions: whole brain, hippocampus, cerebellum, caudate nucleus, putamen, thalamus, and gyrus precentralis. These regions were chosen on the basis of a previous preclinical study (*20*). For comparison of time–activity curves between individual subjects, radioactivity concentrations (kBq/mL) were normalized to injected radiotracer amount and expressed as standardized uptake values (SUVs). Time–activity curves of total radioactivity in whole blood multiplied by individual fractions of blood volume in brain derived from kinetic modeling were used to correct brain time–activity curves for radioactivity in the vascular compartment.

Kinetic Modeling

For ^{11}C-tariquidar and ^{11}C-elacridar, datasets from 0 to 60 min of scan 1 (i.e., before tariquidar administration) were used for analysis. Standard 1-tissue 2-rate-constant (1T2K) and 2-tissue 4-rate-constant (2T4K) compartment models were fitted to the time–activity data of each volume of interest using plasma input functions either uncorrected or corrected for radiolabeled metabolites of ^{11}C-tariquidar and ^{11}C-elacridar. Time delays of 1–4 s were considered in the input functions to account for the differences in the time course of activity between the arterial catheter and the arterial capillaries in the brain. From the fits, rate constants K_1 and k_2 (1T2K model) and rate constants K_1, k_2, k_3, and k_4 (2T4K model), as well as blood volume fraction in brain, were estimated and the V_T of the respective brain volume of interest was calculated. Fits were performed by software developed in-house using the method of weighted nonlinear least squares as implemented in the Optimization Toolbox of MATLAB (MathWorks). The quality of the fits was judged by visual inspection of observed and predicted activities together with the pattern of the residuals, by the correlation between observed and predicted activities, and by estimation of parameter uncertainties (SEs) from the diagonal elements of the covariance matrix as obtained from the inverse of the corresponding Fisher information matrix. Model selection (1T2K vs. 2T4K) was based on the Akaike information criterion (*21*). For (*R*)-^{11}C-verapamil scans, a 2T4K model with plasma input function corrected for polar radiolabeled metabolites was used (*17*). Model outcome parameters obtained with the software developed in-house were cross-checked using the General Kinetic Modeling Tool in PMOD (version 2.6.1; PMOD group).

Analysis of ABCG2 and ABCB1 Single-Nucleotide Polymorphisms

Venous blood (4 mL) was drawn during the screening examination from all study participants for assessment of common ABCG2 and ABCB1 single-nucleotide polymorphisms (SNPs) using previously described procedures (*22,23*). The C421A variant (ABI TaqMan Genotyping Assay C__15854163_70; Applied Biosystems) was determined for ABCG2, and the C1236T, G2677T, and C3435T SNPs were determined for ABCB1.

Statistical Analysis

Statistical analysis was performed using Prism 5.0 software (GraphPad Software). A value of P less than 0.05 was considered significant.

RESULTS

Five subjects underwent ^{11}C-tariquidar and (*R*)-^{11}C-verapamil PET scans, and 1 subject underwent only an ^{11}C-tariquidar PET scan. One subject was excluded from data analysis because of technical problems with generation of the input function of ^{11}C-tariquidar. Five further subjects underwent ^{11}C-elacridar and (*R*)-^{11}C-verapamil PET scans.

There were no adverse or clinically detectable pharmacologic effects related to the radiotracers injected in any of the 11 subjects. Dysgeusia and orthostatic hypotonia occurred as adverse events in 4 and 2 subjects, respectively, and were most likely related to the infusion of unlabeled tariquidar.

After the injection of ^{11}C-tariquidar or ^{11}C-elacridar, brain PET signal was low (~0.1 SUV) and distributed uniformly throughout the brain, with the exception of intense focal uptake in the venous sinus and the choroid plexus (Fig. 2). Time–activity curves for ^{11}C-tariquidar or ^{11}C-elacridar in plasma and whole-brain gray matter are shown in Figure 3. One study subject who was scanned with ^{11}C-elacridar (subject 10) showed 2- to 3-fold higher activity concentrations in plasma and 3- to 4-fold higher activity concentrations in brain (Supplemental Fig. 1) than were seen in the other

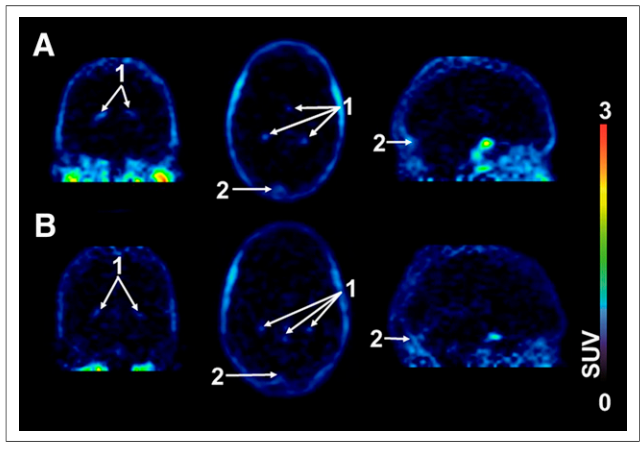

FIGURE 2. Representative PET summation images (0–60 min) of ^{11}C-tariquidar (A) and ^{11}C-elacridar (B) in coronal (left), transaxial (middle), and sagittal views (right). Activity concentration is expressed as SUV, and radiation scale is set from 0 to 3. Anatomic structures are labeled using arrows (1, choroid plexus; 2, venous sinus).

study subjects and was therefore not included in the mean time–activity curves shown in Figure 3. At 60 min after injection of ^{11}C-tariquidar or ^{11}C-elacridar, unlabeled tariquidar was administered as an intravenous infusion over 30 min and PET data acquisition continued for a further 60 min (Fig. 1). In response to tariquidar infusion, there was a small but clearly visible rise in brain PET signal both for ^{11}C-tariquidar and for ^{11}C-elacridar, whereas plasma activity concentrations were essentially unchanged (Fig. 3). The brain PET signal (SUV) of ^{11}C-tariquidar was increased on average by 27% ± 15% (P = 0.014, paired t test) at the end of scan 1, as compared with a time point before tariquidar infusion (45 min), whereas the PET signal of ^{11}C-elacridar was increased by 21% ± 15% (P = 0.014). Interestingly, subject 10 showed only a weak response to tariquidar infusion (+4% increase in brain SUV, Supplemental Fig. 1). Plasma activity concentrations before and after tariquidar infusion were not significantly different between ^{11}C-tariquidar (P = 0.368, paired t test) and ^{11}C-elacridar (P = 0.283). In Supplemental Table 1, tariquidar plasma concentration levels at 4 different time points after tariquidar infusion are given for individual subjects.

Radioactivity in plasma samples collected at time points between 3.5 and 60 min after injection was analyzed for radiolabeled metabolites of ^{11}C-tariquidar and ^{11}C-elacridar using a SPE/HPLC assay. At all studied time points, the fraction of polar radiolabeled metabolites of ^{11}C-tariquidar and ^{11}C-elacridar in plasma was less than 0.25 (Fig. 4). Radio-HPLC analysis of methanol/buffer eluates from the SPE assay did not show any radioactive species other than unchanged parent compound (Supplemental Fig. 2). Plasma–to–whole-blood ratios of total radioactivity over time were rather stable, that is, 1.34 ± 0.08, 1.39 ± 0.12, and 1.36 ± 0.08 at, respectively, 3.5, 30, and 60 min after injection of ^{11}C-tariquidar (n = 5) and 1.51 ± 0.10, 1.51 ± 0.12, and 1.48 ± 0.10 at the same respective time points after injection of ^{11}C-elacridar (n = 5).

Data were modeled using 1T2K and 2T4K models with plasma input functions either uncorrected (Table 1) or corrected (Supplemental Table 2) for radiolabeled metabolites. The 2T4K model provided better fits (i.e., lower Akaike information criterion values) than the 1T2K model. Representative 2T4K model fits for whole brain are shown in Figure 5. K_4 values in the 2T4K model were low, pointing to partially irreversible behavior (Table 1). Outcome parameters were similar when metabolite-corrected or uncorrected input functions were used and supported the notion that the influence of radiolabeled metabolites on radiotracer kinetics

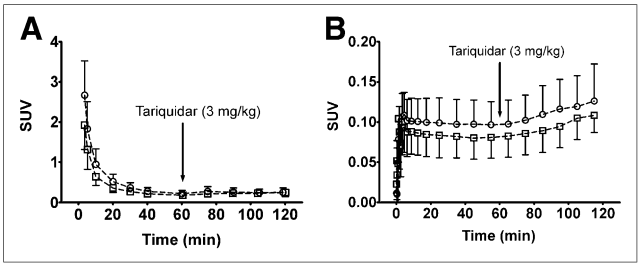

FIGURE 3. Time–activity curves (mean SUV ± SD) of ^{11}C-tariquidar (□, n = 5) and ^{11}C-elacridar (○, n = 4, subject 10 not included) in arterial plasma, uncorrected for radiolabeled metabolites (A), and in whole-brain gray matter, corrected for radioactivity in vasculature (B). Start of intravenous tariquidar infusion (3 mg/kg, over 30 min) is indicated by arrow.

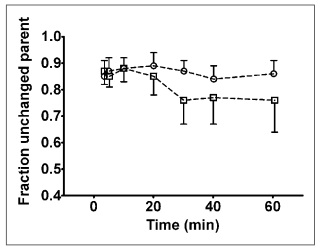

FIGURE 4. Fractions (mean ± SD) of unchanged ^{11}C-tariquidar (□, n = 5) and ^{11}C-elacridar (○, n = 5) in arterial plasma over time as determined by SPE assay. Shown values are not corrected for recoveries of ^{11}C-tariquidar and ^{11}C-elacridar, which ranged from 91% to 94%.

was negligible. The V_T and K_1 values of subject 10 in whole brain were approximately 1.5-fold above average (2T4K: K_1, 0.007; V_T, 0.51), whereas other outcome parameters were within the reference range.

Regional 2T4K model-derived V_Ts of ^{11}C-tariquidar and ^{11}C-elacridar are shown in Figure 6. There was no statistically significant correlation between the V_Ts of ^{11}C-tariquidar or ^{11}C-elacridar and the V_Ts of (*R*)-^{11}C-verapamil in different brain regions (Fig. 7). All study participants were genotyped for common functional SNPs of ABCG2 and ABCB1 (Supplemental Table 3). Subject 10 was a homozygous carrier of the TTT haplotype (1236T, 2677T, 3435T) in the ABCB1 gene but carried the wild-type ABCG2 C421A allele.

DISCUSSION

This study is, to our knowledge, the first to describe the brain distribution and pharmacokinetics of radiolabeled third-generation Pgp inhibitors in humans. We found that the brain PET signal of ^{11}C-tariquidar and ^{11}C-elacridar, when administered in tracer doses, was low (Fig. 2), as was consistent with previous in vitro and in vivo data suggesting that these substances are concentration-dependently transported by Pgp and BCRP at the BBB (*6–11,16*).

In analogy to a recent human PET study with (*R*)-^{11}C-verapamil (*17*), we administered unlabeled tariquidar during the ^{11}C-tariquidar and ^{11}C-elacridar PET scans (Fig. 1). Administration of Pgp inhibitor during the PET scan has been shown to allow for detection of Pgp efflux transport of a radiotracer at the BBB (*24*). The used tariquidar dose (3 mg/kg), when given 1 h before the start of the PET scan, corresponded to the half-maximum-effect dose for inhibition of Pgp at the human BBB (*18*). Despite our use of a higher tariquidar dose in this study than in the previous (*R*)-^{11}C-verapamil study (2 mg/kg), we observed a much less pronounced rise in brain PET signal of ^{11}C-tariquidar and ^{11}C-elacridar in response to tariquidar than for (*R*)-^{11}C-verapamil (Fig. 3). The most likely explanation for this different behavior could be that (*R*)-^{11}C-verapamil is transported only by Pgp at the human BBB whereas ^{11}C-tariquidar and ^{11}C-elacridar are dual Pgp/BCRP substrates. Even though tariquidar in pharmacologic doses is a dual Pgp and BCRP inhibitor, preclinical data suggest that higher doses than the presently used 3 mg/kg dose would be needed to inhibit BCRP (*16*). Therefore it can be assumed that although Pgp was at least half-maximally inhibited, BCRP was still fully functional during administration of a 3 mg/kg dose of tariquidar and that BCRP efflux may have effectively limited brain access of both radiotracers. This behavior is in fact completely in line with what would be expected from dual Pgp/BCRP substrates (*2*). It has now been documented in the literature for several dual Pgp/BCRP substrates that their brain uptake is only moderately increased in single-transporter knockout mice, that is, Mdr1a/b$^{(-/-)}$ or Bcrp1$^{(-/-)}$ mice, relative to wild-type mice, whereas dispropor-

TABLE 1
Outcome Parameters for Whole-Brain Gray Matter of 1T2K and 2T4K Models* for ^{11}C-Tariquidar and ^{11}C-Elacridar

	1T2K		2T4K	
Parameter	^{11}C-tariquidar	^{11}C-elacridar	^{11}C-tariquidar	^{11}C-elacridar
K_1 (mL·mL^{-1}·min^{-1})	0.003 ± 0.001 (0.002–0.004)	0.003 ± 0.001 (0.002–0.003)	0.004 ± 0.001 (0.003–0.004)	0.005 ± 0.001 (0.004–0.005)
k_2 (min^{-1})	0.013 ± 0.003 (0.010–0.016)	0.012 ± 0.003 (0.009–0.014)	0.076 ± 0.023 (0.055–0.097)	0.124 ± 0.031 (0.094–0.155)
k_3 (min^{-1})			0.100 ± 0.031 (0.073–0.127)	0.108 ± 0.032 (0.076–0.140)
k_4 (min^{-1})			0.016 ± 0.007 (0.010–0.022)	0.014 ± 0.006 (0.007–0.020)
V_T (mL·mL^{-1})	0.23 ± 0.04 (0.20–0.27)	0.24 ± 0.09 (0.15–0.33)	0.35 ± 0.07 (0.29–0.42)	0.36 ± 0.07 (0.29–0.43)
V_b	0.050 ± 0.008 (0.043–0.057)	0.046 ± 0.003 (0.042–0.049)	0.046 ± 0.006 (0.042–0.051)	0.042 ± 0.003 (0.038–0.045)
AIC	−34.1 ± 8.5	−33.8 ± 7.7	−42.2 ± 6.3	−49.7 ± 1.9

*Data from 0 to 60 min were used, and plasma input function was not corrected for radiolabeled metabolites.
K_1, k_2, k_3, and k_4 = rate constants for exchange of radioactivity between plasma and brain compartments; V_b = blood volume fraction in brain; AIC = Akaike information criterion.
Outcome parameters are given as mean ± SD (^{11}C-tariquidar: n = 5, ^{11}C-elacridar: n = 4, subject 10 excluded). In parentheses, 95% confidence intervals of mean parameter estimates are given.

tionally large increases are seen in combination knockout mice (Mdr1a/b$^{(-/-)}$Bcrp1$^{(-/-)}$) (*1*). This observation is because of a cooperative effect of both transporters in preventing brain distribution of dual substrates (*1*). In line with this finding, brain-to-blood ratios of ^{11}C-tariquidar were found to be 1.0 ± 0.1 in wild-type, 3.3 ± 0.4 in Mdr1a/b$^{(-/-)}$, 1.8 ± 0.1 in Bcrp1$^{(-/-)}$, and 14.4 ± 1.7 in Mdr1a/b$^{(-/-)}$Bcrp1$^{(-/-)}$ mice (*9*).

We used 1T2K and 2T4K models for analysis and found that the 2T4K model provided better data fits (Fig. 5; Table 1). Importantly, the fact that we observed only low levels of radiolabeled metabolites of ^{11}C-tariquidar and ^{11}C-elacridar in plasma during the time course of the PET scan (Fig. 4 and Supplemental Fig. 2) obviates correction of plasma input functions for radiolabeled metabolites. This poses a significant advantage over (*R*)-^{11}C-verapamil, which is extensively metabolized and gives radiolabeled metabolites, which are partly taken up into brain and may thereby confound PET measurements with this radiotracer (*25*). K_1 values of ^{11}C-tariquidar and ^{11}C-elacridar were up to 10-fold lower than those of (*R*)-^{11}C-verapamil (Table 1) (*17*), suggesting that ^{11}C-tariquidar and ^{11}C-elacridar underwent efflux more effectively at the BBB than (*R*)-^{11}C-verapamil. Washout of ^{11}C-tariquidar and ^{11}C-elacridar from the brain was slow (Fig. 3). The good fits obtained with the 2T4K model (Fig. 5) suggest the presence of a second, deep, brain compartment, the physiologic correlate of which may be intracellular trapping of radiotracer in lysosomes, as recently reported for tariquidar (*26*).

Interestingly, subject 10 had approximately 1.5-fold higher V_T and K_1 values of ^{11}C-elacridar than the other subjects. Genetic analysis revealed that this subject was a homozygous carrier of the TTT haplotype in the ABCB1 gene, which has been associated in some studies with decreased Pgp expression and function and altered pharmacokinetics of Pgp substrate drugs (*27*). Thus, it is tempting to speculate that increased brain distribution of ^{11}C-elacridar in subject 10 may have been caused by decreased Pgp function at the BBB, although this finding needs to be confirmed in a larger cohort.

The original intention of developing ^{11}C-tariquidar and ^{11}C-elacridar was to visualize Pgp expression levels in brain. To investigate any possible Pgp binding of ^{11}C-tariquidar and ^{11}C-elacridar at the BBB, we combined ^{11}C-tariquidar and ^{11}C-elacridar PET scans with (*R*)-^{11}C-verapamil scans, after administration of a 3 mg/kg dose of tariquidar. We have shown previously that (*R*)-^{11}C-verapamil PET scanning after half-maximal inhibition of Pgp is more sensitive to map regional differences in cerebral Pgp function than baseline scans (*20*), because brain uptake of (*R*)-^{11}C-verapamil is relatively low in baseline scans, which may make it difficult to detect any further reduction in brain uptake due to regionally increased Pgp activity. Moreover, half-maximal Pgp inhibition may increase the percentage of (*R*)-^{11}C-verapamil in the brain relative to its radiolabeled metabolites, which are not or are to a lower extent transported by Pgp (*25*), thereby providing better sensitivity for studying regional Pgp function in the brain. If ^{11}C-tariquidar and ^{11}C-elacridar bind to Pgp and (*R*)-^{11}C-verapamil undergoes efflux by Pgp, brain uptake of ^{11}C-inhibitors and ^{11}C-substrates should in theory be inversely related; that is, brain regions with high uptake of ^{11}C-inhibitor should show low uptake of ^{11}C-substrate and vice versa. Such a behavior has in fact been observed in a study on rats in which the same paired-scan protocol was used as in the present study (*13*). Contrary to these preclinical results, we found no significant correlation between regional brain V_Ts of ^{11}C-tariquidar or ^{11}C-elacridar and (*R*)-^{11}C-verapamil

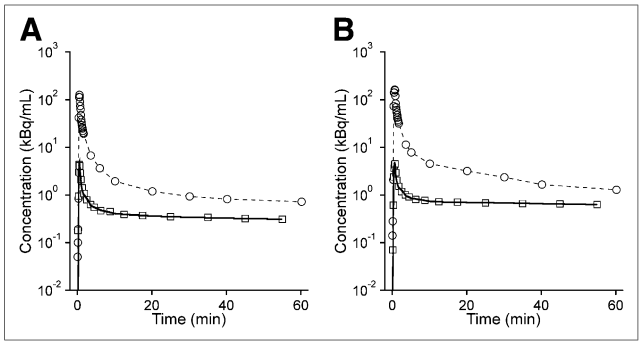

FIGURE 5. Representative fits (solid lines) from 2T4K model using plasma input functions uncorrected for radiolabeled metabolites (○) for whole-brain gray matter (□) for ^{11}C-tariquidar (A) and ^{11}C-elacridar (B).

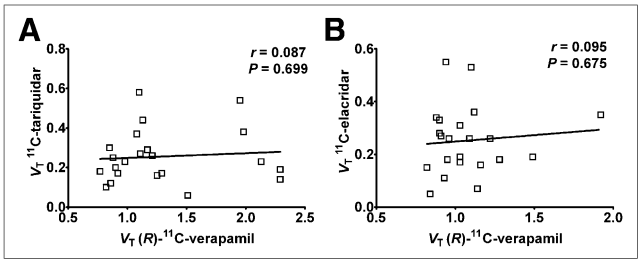

FIGURE 7. Correlation of V_Ts of ^{11}C-tariquidar (A, $n = 5$) and ^{11}C-elacridar (B, $n = 4$, subject 10 not included) (using 2T4K model and plasma input function uncorrected for radiolabeled metabolites) with V_Ts of (*R*)-^{11}C-verapamil in hippocampus, cerebellum, caudate nucleus, putamen, thalamus, and gyrus precentralis. Solid lines represent linear regression fits (r = Pearson correlation coefficient).

(Fig. 7). This lack of correlation strongly suggests that other than at the rodent BBB, where both ^{11}C-tariquidar and ^{11}C-elacridar appeared to undergo efflux by Pgp and also to bind to some extent to Pgp, possibly via distinct binding sites, the behavior of these probes at the human BBB is dominated by Pgp/BCRP efflux. A possible reason could be species-dependent differences in transporter expression levels at the human and rodent BBB. Shortly after we developed ^{11}C-elacridar and ^{11}C-tariquidar, data on absolute Pgp expression levels in isolated brain microvessels of various species, including humans, appeared in the literature (*28*). Using an LC/MS-based quantitative proteomics approach, the expression of MDR1 in isolated human brain microvessels was found to be 2.3-fold lower than that of mdr1a in mouse brain microvessels (6.1 ± 1.7 vs. 14.1 ± 2.1 fmol/μg of protein) (*28*). A commonly used predictor for the magnitude of specific signal that can be obtained with a radioligand for imaging of a molecular target is the ratio of the concentration of target protein in whole brain (B_{max}) to the equilibrium dissociation constant (K_D) of the radioligand (*29*). B_{max}/K_D is also referred to as binding potential and should ideally be greater than 5 to achieve measurable specific binding. To estimate the B_{max} of Pgp in whole brain, one needs to know the density of brain capillary endothelial cells as a proportion of brain tissue. This value is different from total brain capillary volume (~5%), which is much higher because it includes blood volume. Assuming a brain capillary endothelial cell volume of 0.2% of total brain volume (*30*) and a protein content of brain capillaries of 10%, the B_{max} of Pgp in human brain is 1.3 nM. On the basis of a K_D value for binding of ^{3}H-tariquidar to Chinese hamster ovary resistant cells of 5.1 nM (*4*), the binding potential is 0.26, which is clearly too low to visualize Pgp in the human brain with ^{11}C-tariquidar. Another factor that might contribute to the inability of ^{11}C-tariquidar and ^{11}C-elacridar to visualize Pgp density in the human brain could be that BCRP expression levels and BCRP/Pgp expression ratios are higher at the human than at the rodent BBB (BCRP expression [fmol/μg of protein]: humans, 8.14 ± 2.26; mouse, 4.41 ± 0.69; BCRP/Pgp expression ratio: humans, 1.3; mouse, 0.3) (*28*). Thus, a relatively higher contribution of BCRP efflux at the human than at the rodent BBB could further reduce any possible Pgp binding of ^{11}C-tariquidar and ^{11}C-elacridar at the human BBB. In contrast to the BBB, Pgp density in the previously investigated murine tumor model may have been higher and BCRP density lower, as could explain, possibly in combination with the absence of tight junctions in tumor capillaries, why ^{11}C-tariquidar was able to visualize Pgp expression in the tumor model (*12*). More generally, the ability of ^{11}C-tariquidar and ^{11}C-elacridar to provide a Pgp-binding signal may be tissue-specific, depending on Pgp relative to BCRP expression levels. Following these considerations, an effective radioligand to visualize Pgp density in the human brain should ideally possess an at least 10-fold higher Pgp binding affinity than tariquidar and not be transported by BCRP and Pgp.

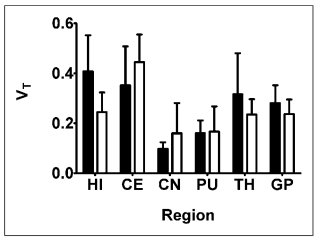

FIGURE 6. Mean (+SD) 2T4K model-derived V_T values (using plasma input function uncorrected for radiolabeled metabolites) for ^{11}C-tariquidar (black bars, $n = 5$) and ^{11}C-elacridar (white bars, $n = 4$, subject 10 not included) in different brain regions. HI = hippocampus; CE = cerebellum; CN = caudate nucleus; PU = putamen; TH = thalamus; GP = gyrus precentralis.

Despite the inability of ^{11}C-tariquidar and ^{11}C-elacridar to visualize cerebral Pgp density, these probes may find use as an entirely new class of PET tracers (as opposed to Pgp-selective substrates such as (*R*)-^{11}C-verapamil or ^{11}C-*N*-desmethyl-loperamide) to study the interplay of Pgp and BCRP at the human BBB in limiting brain uptake of dual substrates (*16*). This use would be important because several clinically applied drugs (e.g., tyrosine kinase inhibitors) are dual substrates of Pgp and BCRP (*1*) and no dual Pgp/BCRP substrates are currently available for PET studies in humans. Thus, ^{11}C-tariquidar or ^{11}C-elacridar could be used as generic probes to assess brain penetration of dual Pgp/BCRP substrates in healthy subjects or glioma patients under various conditions—for example, after treatment with Pgp/BCRP inhibitors such as elacridar or in subjects with functional SNPs in the ABCG2 or ABCB1 genes.

CONCLUSION

The brain PET signal of ^{11}C-tariquidar and ^{11}C-elacridar was found to be low in humans and only moderately sensitive to a pharmacologic challenge with unlabeled tariquidar, consistent with the behavior of dual Pgp/BCRP substrates. ^{11}C-tariquidar and ^{11}C-elacridar were not able to visualize Pgp density in the human brain, thus highlighting the considerable challenge in visualizing low-density multidrug efflux transporters at the human

BBB with PET and furthermore suggesting that compounds with subnanomolar Pgp binding affinities, which are currently not available, may be needed to develop successful radioligands. Despite their inability to visualize Pgp density, ^{11}C-tariquidar and ^{11}C-elacridar may find future clinical use as an entirely new class of radiotracers to assess the interplay of Pgp and BCRP at the human BBB.

DISCLOSURE

The costs of publication of this article were defrayed in part by the payment of page charges. Therefore, and solely to indicate this fact, this article is hereby marked "advertisement" in accordance with 18 USC section 1734. This study was supported by the European Community's Seventh Framework program (grant 201380) and the Austrian Science Fund (FWF) (grant F 3513-B20). No other potential conflict of interest relevant to this article was reported.

ACKNOWLEDGMENTS

We thank Georgios Karanikas and the staff of the PET center at the Department of Nuclear Medicine and Research Nurse Maria Weber for their support in performing this study, Elisabeth Ponweiser and Raute Sunder-Plassmann for analysis of ABCB1 SNPs, and Michaela Böhmdorfer for measurement of tariquidar plasma concentrations. Divya Maheshwari (AzaTrius Pharmaceuticals Pvt. Ltd.) is acknowledged for providing tariquidar for intravenous injection, Joseph W. Polli (GlaxoSmithKline, Inc.) for providing the Investigator's Brochure for elacridar, and Marie-Claude Asselin from the Wolfson Molecular Imaging Centre (Manchester, U.K.) for providing valuable input into kinetic modeling of PET data.

REFERENCES

1. Agarwal S, Hartz AM, Elmquist WF, Bauer B. Breast cancer resistance protein and P-glycoprotein in brain cancer: two gatekeepers team up. *Curr Pharm Des.* 2011;17:2793–2802.
2. Kodaira H, Kusuhara H, Ushiki J, Fuse E, Sugiyama Y. Kinetic analysis of the cooperation of P-glycoprotein (P-gp/Abcb1) and breast cancer resistance protein (Bcrp/Abcg2) in limiting the brain and testis penetration of erlotinib, flavopiridol, and mitoxantrone. *J Pharmacol Exp Ther.* 2010;333:788–796.
3. Szakács G, Paterson JK, Ludwig JA, Booth-Genthe C, Gottesman MM. Targeting multidrug resistance in cancer. *Nat Rev Drug Discov.* 2006;5:219–234.
4. Martin C, Berridge G, Mistry P, Higgins C, Charlton P, Callaghan R. The molecular interaction of the high affinity reversal agent XR9576 with P-glycoprotein. *Br J Pharmacol.* 1999;128:403–411.
5. Kannan P, John C, Zoghbi SS, et al. Imaging the function of P-glycoprotein with radiotracers: pharmacokinetics and in vivo applications. *Clin Pharmacol Ther.* 2009;86:368–377.
6. Kawamura K, Yamasaki T, Konno F, et al. Evaluation of limiting brain penetration related to P-glycoprotein and breast cancer resistance protein using [^{11}C]GF120918 by PET in mice. *Mol Imaging Biol.* 2011;13:152–160.
7. Kawamura K, Konno F, Yui J, et al. Synthesis and evaluation of [^{11}C]XR9576 to assess the function of drug efflux transporters using PET. *Ann Nucl Med.* 2010;24:403–412.
8. Dörner B, Kuntner C, Bankstahl JP, et al. Synthesis and small-animal positron emission tomography evaluation of [^{11}C]-elacridar as a radiotracer to assess the distribution of P-glycoprotein at the blood-brain barrier. *J Med Chem.* 2009;52:6073–6082.
9. Bauer F, Kuntner C, Bankstahl JP, et al. Synthesis and in vivo evaluation of [^{11}C]tariquidar, a positron emission tomography radiotracer based on a third-generation P-glycoprotein inhibitor. *Bioorg Med Chem.* 2010;18:5489–5497.
10. Bankstahl JP, Bankstahl M, Römermann K, et al. Tariquidar and elacridar are dose-dependently transported by P-glycoprotein and Bcrp at the blood-brain barrier: a small-animal PET and in-vitro study. *Drug Metab Dispos.* 2013;41:754–762.
11. Kannan P, Telu S, Shukla S, et al. The "specific" P-glycoprotein inhibitor tariquidar is also a substrate and an inhibitor for breast cancer resistance protein (BCRP/ABCG2). *ACS Chem Neurosci.* 2011;2:82–89.
12. Wanek T, Kuntner C, Bankstahl JP, et al. A comparative small-animal PET evaluation of [^{11}C]tariquidar, [^{11}C]elacridar and (R)-[^{11}C]verapamil for detection of P-glycoprotein-expressing murine breast cancer. *Eur J Nucl Med Mol Imaging.* 2012;39:149–159.
13. Müllauer J, Karch R, Bankstahl JP, et al. Assessment of cerebral P-glycoprotein expression and function with PET by combined [^{11}C]inhibitor and [^{11}C]substrate scans in rats. *Nucl Med Biol*. June 15, 2013 [Epub ahead of print].
14. Langer O, Bauer M, Hammers A, et al. Pharmacoresistance in epilepsy: a pilot PET study with the P-glycoprotein substrate R-[^{11}C]verapamil. *Epilepsia.* 2007;48:1774–1784.
15. Wang SW, Monagle J, McNulty C, Putnam D, Chen H. Determination of P-glycoprotein inhibition by excipients and their combinations using an integrated high-throughput process. *J Pharm Sci.* 2004;93:2755–2767.
16. Wanek T, Kuntner C, Bankstahl JP, et al. A novel PET protocol for visualization of breast cancer resistance protein function at the blood-brain barrier. *J Cereb Blood Flow Metab.* 2012;32:2002–2011.
17. Wagner CC, Bauer M, Karch R, et al. A pilot study to assess the efficacy of tariquidar to inhibit P-glycoprotein at the human blood-brain barrier with (R)-^{11}C-verapamil and PET. *J Nucl Med.* 2009;50:1954–1961.
18. Bauer M, Zeitlinger M, Karch R, et al. Pgp-mediated interaction between (R)-[^{11}C]verapamil and tariquidar at the human blood-brain barrier: a comparison with rat data. *Clin Pharmacol Ther.* 2012;91:227–233.
19. Hammers A, Allom R, Koepp MJ, et al. Three-dimensional maximum probability atlas of the human brain, with particular reference to the temporal lobe. *Hum Brain Mapp.* 2003;19:224–247.
20. Bankstahl JP, Bankstahl M, Kuntner C, et al. A novel PET imaging protocol identifies seizure-induced regional overactivity of P-glycoprotein at the blood-brain barrier. *J Neurosci.* 2011;31:8803–8811.
21. Akaike H. An information criterion (AIC). *Math Sci.* 1976;14:5–9.
22. Hui L, DelMonte T, Ranade K. Genotyping using the TaqMan assay. *Curr Protoc Hum Genet.* 2008;chapter 2:unit 2.10.
23. Sunder-Plassmann R, Rieger S, Endler G, Brunner M, Müller M, Mannhalter C. Simultaneous analysis of MDR1 C3435T, G2677T/A, and C1236T genotypes by multiplexed mutagenically separated PCR. *Clin Chem Lab Med.* 2005;43:192–194.
24. Syvänen S, Blomquist G, Sprycha M, et al. Duration and degree of cyclosporin induced P-glycoprotein inhibition in the rat blood-brain barrier can be studied with PET. *Neuroimage.* 2006;32:1134–1141.
25. Lubberink M, Luurtsema G, van Berckel BN, et al. Evaluation of tracer kinetic models for quantification of P-glycoprotein function using (R)-[^{11}C]verapamil and PET. *J Cereb Blood Flow Metab.* 2007;27:424–433.
26. Kannan P, Brimacombe KR, Kreisl WC, et al. Lysosomal trapping of a radiolabeled substrate of P-glycoprotein as a mechanism for signal amplification in PET. *Proc Natl Acad Sci USA.* 2011;108:2593–2598.
27. Cascorbi I. Role of pharmacogenetics of ATP-binding cassette transporters in the pharmacokinetics of drugs. *Pharmacol Ther.* 2006;112:457–473.
28. Uchida Y, Ohtsuki S, Katsukura Y, et al. Quantitative targeted absolute proteomics of human blood-brain barrier transporters and receptors. *J Neurochem.* 2011;117:333–345.
29. Eckelman WC, Mathis CA. Targeting proteins in vivo: in vitro guidelines. *Nucl Med Biol.* 2006;33:161–164.
30. Pardridge WM. Blood-brain barrier biology and methodology. *J Neurovirol.* 1999;5:556–569.